BAMS Article

S-MODE: The Sub-Mesoscale Ocean Dynamics Experiment

J. Thomas Farrar,[a] Eric D'Asaro,[b] Ernesto Rodríguez,[c] Andrey Shcherbina,[b] Luc Lenain,[d] Melissa Omand,[e] Alex Wineteer,[c] Paban Bhuyan,[f] Fred Bingham,[g] A. B. Villas Boas,[h] Erin Czech,[i] Joseph D'Addezio,[j] Mara Freilich,[k] Laurent Grare,[d] Delphine Hypolite,[l] Gregg Jacobs,[j] Patrice Klein,[c] Sarah Lang,[e] Inés M. Leyba,[m] Zhijin Li,[l] Amala Mahadevan,[a] James McWilliams,[l] Dimitris Menemenlis,[c] Leo Middleton,[a] Jeroen Molemaker,[l] Larry O'Neill,[m] Dragana Perkovic-Martin,[c] Nick Pizzo,[e] Luc Rainville,[b] Cesar Rocha,[n] R. M. Samelson,[m] Iury Simoes-Sousa,[a] Nick Statom,[d] Andrew Thompson,[o] David Thompson,[c] Hector Torres,[c] Igor Uchoa,[p] Jacob Wenegrat,[p] and Elizabeth Westbrook[g]

KEYWORDS:
Ocean dynamics;
Atmosphere-ocean interaction;
Eddies;
Aircraft observations;
In situ oceanic observations

ABSTRACT: The Sub-Mesoscale Ocean Dynamics Experiment (S-MODE) is a NASA Earth Ventures Suborbital investigation designed to test the hypothesis that oceanic frontogenesis and the kilometer-scale ("submesoscale") instabilities that accompany it make important contributions to vertical exchange of climate and biological variables in the upper ocean. These processes have been difficult to resolve in observations, making model validation challenging. A necessary step toward testing the hypothesis was to make accurate measurements of upper-ocean velocity fields over a broad range of scales and to relate them to the observed variability of vertical transport and surface forcing. A further goal was to examine the relationship between surface velocity, temperature, and chlorophyll measured by remote sensing and their depth-dependent distributions, within and beneath the surface boundary layer. To achieve these goals, we used aircraft-based remote sensing, satellite remote sensing, ships, drifter deployments, and a fleet of autonomous vehicles. The observational component of S-MODE consisted of three campaigns, all conducted in the Pacific Ocean approximately 100-km west of San Francisco during 2021–23 fall and spring. S-MODE was enabled by recent developments in remote sensing technology that allowed operational airborne observation of ocean surface velocity fields and by advances in autonomous instrumentation that allowed coordinated sampling with dozens of uncrewed vehicles at sea. The coordinated use of remote sensing measurements from three aircraft with arrays of remotely operated vehicles and other in situ measurements is a major novelty of S-MODE. All S-MODE data are freely available, and their use is encouraged.

DOI: 10.1175/BAMS-D-23-0178.1
Corresponding author: J. Thomas Farrar, jfarrar@whoi.edu
Manuscript received 14 July 2023, in final form 21 January 2025, accepted 11 February 2025

SIGNIFICANCE STATEMENT: S-MODE is a NASA Earth Venture Suborbital investigation that combines novel aircraft remote sensing techniques with coordinated measurements from ships and a fleet of uncrewed vehicles and other measurement platforms to study submesoscale ocean dynamics (scales less than about 10 km) and their contribution to vertical transport in the upper ocean. Oceanic fronts and the submesoscale instabilities that develop on them are thought to be important for vertical transport in the upper ocean, but these rapidly evolving features have been difficult to observe in detail. High-resolution computational models produce the features, but they need to be checked against observations. S-MODE addresses these challenges with coordinated sampling from three research aircraft, a research vessel, and dozens of uncrewed surface and subsurface platforms.

AFFILIATIONS: [a] Woods Hole Oceanographic Institution, Woods Hole, Massachusetts; [b] Applied Physics Laboratory, University of Washington, Seattle, Washington; [c] Jet Propulsion Laboratory, California Institute of Technology, Pasadena, California; [d] Scripps Institution of Oceanography, La Jolla, California; [e] Graduate School of Oceanography, University of Rhode Island, Narragansett, Rhode Island; [f] University of Connecticut, Groton, Connecticut; [g] University of North Carolina, Wilmington, North Carolina; [h] Colorado School of Mines, Golden, Colorado; [i] NASA Ames Research Center, Mountain View, California; [j] U.S. Naval Research Laboratory, John C. Stennis Space Center, Mississippi; [k] Brown University, Providence, Rhode Island; [l] University of California, Los Angeles, Los Angeles, California; [m] Oregon State University, Corvallis, Oregon; [n] Universidade de São Paulo, São Paulo, Brazil; [o] California Institute of Technology, Pasadena, California; [p] University of Maryland, College Park, College Park, Maryland

1. Introduction

Over the last few decades, scientists have come to understand that the upper ocean is full of submesoscale fronts and eddies at scales of 10 km and less (see reviews by Thomas et al. 2008; McWilliams 2016; Mahadevan 2016; Taylor and Thompson 2023). These submesoscale eddies are hypothesized to play an important role in the vertical transport in the ocean surface layer that links the atmosphere to the deep ocean (Siegelman et al. 2020), mediating atmosphere–ocean exchanges of important properties like heat, nutrients, oxygen, and carbon. NASA astronauts collected early and compelling observations of submesoscale eddies in the ocean. After photographs from the Apollo space missions suggested that ocean dynamics were more complicated than generally believed, NASA decided to send an oceanographer on the Space Shuttle *Challenger* Mission STS41G in 1984 (Fig. 1). Paul Scully-Power, the oceanographer–astronaut, proclaimed while flying over the North Pacific (Scully-Power 1986, p. 29), "We're several hundred miles from the California coast . . . once again you continue to see these spiral structures . . . maybe the whole ocean is like this."

NASA has continued to pioneer our understanding of these eddies and their impacts, sponsoring the Earth Ventures Suborbital investigation called the Sub-Mesoscale Ocean Dynamics Experiment (S-MODE) to conduct major field campaigns in 2021–23 to study the dynamics of these submesoscale eddies. S-MODE is using newly developed in situ and remote sensing techniques to study submesoscale eddies and fronts and their contributions to vertical transport in the upper ocean. The $30M, 6-yr mission (2019–25) conducted three separate monthlong field campaigns offshore of San Francisco, using three aircraft, oceanographic research vessels, dozens of uncrewed ocean vehicles, and satellite measurements.

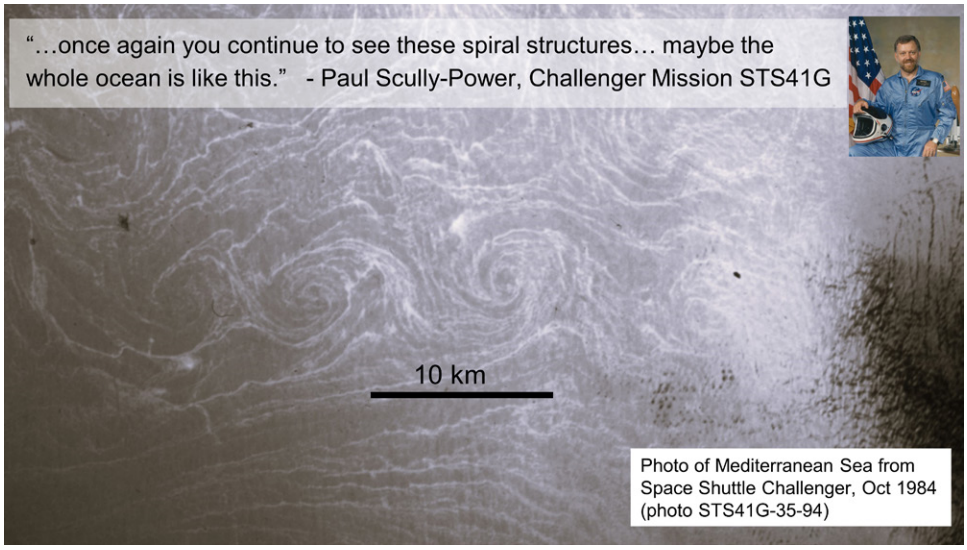

Fig. 1. Background: a photograph taken from the Space Shuttle *Challenger* by oceanographer–astronaut Paul Scully-Power over the Mediterranean Sea in 1984 showing early observations of submesoscale eddies (photo STS41G-35-94; after Fig. 2 of Munk et al. 2000). Inset: photograph of Paul Scully-Power (image credit: NASA).

Our understanding of the dynamics of submesoscale motions and the associated vertical exchange comes primarily from numerical simulations and theory. The distinctive features of the submesoscale—sharp fronts with high vorticity and associated large vertical velocities—typically occur at the smallest scales resolved by the models. Their amplitudes are thus sensitive to resolution and to the details of the numerics and damping at the grid scale (Uchida et al. 2022). Increasing the resolution toward 100 m intensifies the submesoscale features (Fig. 2), but this also brings the computational grid to the same scales as the parameterized boundary layer turbulence. Models and theory indicate both that submesoscale motions are sensitive to the boundary layer turbulence (e.g., "turbulent thermal wind"; McWilliams 2016) and that the boundary layer turbulence itself is affected by the submesoscale gradients (D'Asaro et al. 2011; Sullivan and McWilliams 2024). These effects are only partially included in the state-of-the-art, realistic models.

Submesoscale motions evolve rapidly and have scales large enough that they are difficult to measure with a research vessel moving at 2–5 m s^{-1}. They are too small for many satellite remote sensing techniques, and they evolve too quickly to remain coherent from one satellite pass to the next. The observational approaches of the last couple of decades have focused on measuring statistics of horizontal velocity gradients (vorticity, strain, and divergence) and scalars (e.g., temperature) at submesoscales (e.g., Rudnick 2001; Shcherbina et al. 2013; Callies and Ferrari 2013). For example, Shcherbina et al. (2013) used two research vessels, driven along parallel tracks for 2 days, to obtain a single 500-km line of data on ocean velocity gradients that has been used as a benchmark for evaluating the statistics of submesoscale-resolving models. The low-order statistics provided by these studies (variances, spectra, and probability distributions of quantities like velocity and vorticity) do not provide the information that we need to examine the dynamics and net effects of submesoscale variability. We would like to be able to know the vertical and horizontal *fluxes* of quantities like heat and density, which requires estimates of the covariances of quantities like velocity and temperature.

Over the last decade, new instrumentation and techniques have been developed to overcome the difficulties in observing submesoscale dynamics. Recent observational programs, such as the Coherent Lagrangian Pathways from the Surface Ocean to Interior (CALYPSO) program (Mahadevan et al. 2020), have begun to address the observational gap with estimates of submesoscale vertical velocity from arrays of platforms (e.g., Rudnick et al. 2022;

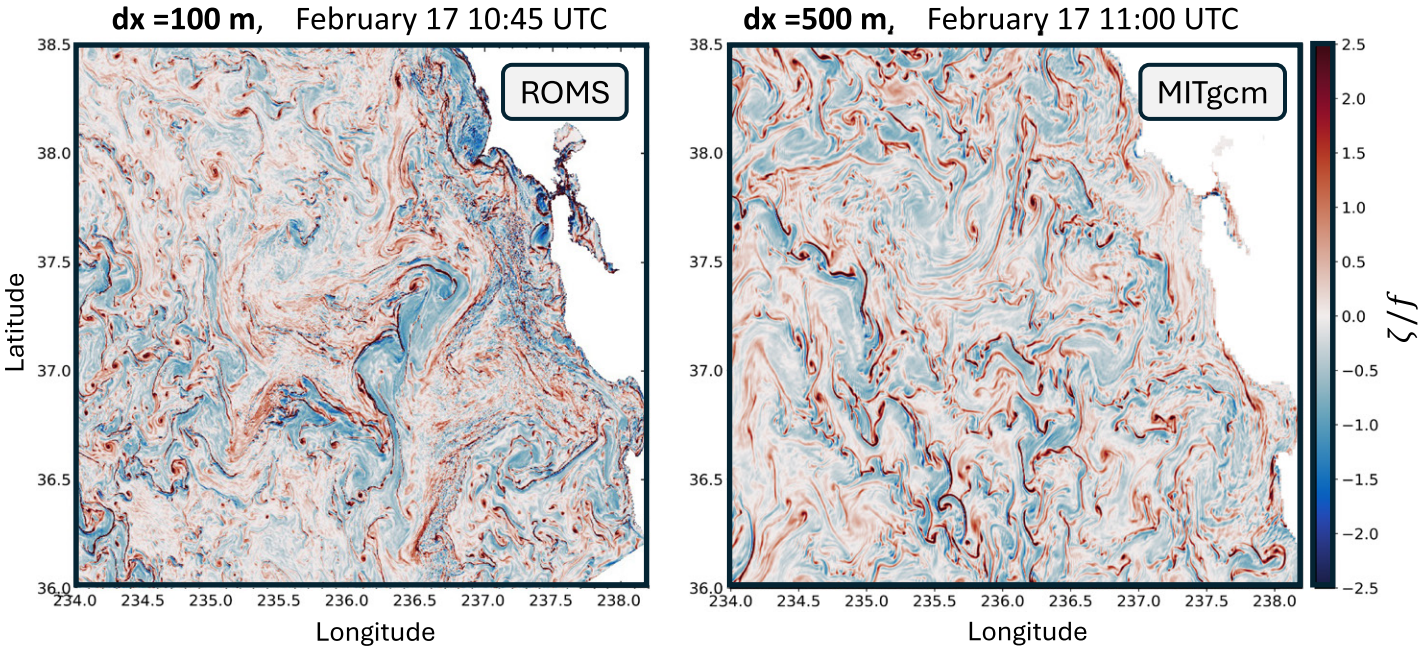

Fig. 2. Snapshot images of surface vertical vorticity normalized by the Coriolis frequency *f* in two nested-grid simulations for the S-MODE region in late winter (more detail in section 2). The left panel used the ROMS and has a horizontal grid resolution of 200 m and high-frequency wind and tidal forcings. The right panel used the MITgcm and has a horizontal grid resolution of 500 m and high-frequency wind and tidal forcings. The intense features are intermittent submesoscale surface fronts, filaments, and cyclonic vortices, while the broader background pattern is of weaker mesoscale eddies.

Tarry et al. 2022). NASA's Earth Venture Suborbital program provided the opportunity to combine multiple, diverse platforms to enable measurements across a range of time and space scales. A central element of the S-MODE experimental design was the recently developed airborne DopplerScatt instrument for simultaneous remote sensing of surface currents and winds (Rodríguez et al. 2018; Wineteer et al. 2020b). A secondary goal of the project was to improve the understanding of the relation between the surface velocity measured by DopplerScatt and the velocity within the ocean surface boundary layer (upper tens of meters), in support of planning for a prospective space-based "ODYSEA" Doppler scatterometer mission (Rodríguez et al. 2019; Villas Bôas et al. 2019; Wineteer et al. 2020b,a; Torres et al. 2023).

This article summarizes the motivation, planning, and execution of the S-MODE program, along with its instruments and three main campaigns.

2. S-MODE experimental design and organization

The experimental design of S-MODE used new remote sensing techniques and the combination of multiple, fast-moving aircraft with a ship and a fleet of autonomous platforms to address the sampling challenges posed by the spatial and temporal variability of submesoscale motions. Airplanes rapidly sampled surface properties over large areas, while uncrewed, remotely piloted vehicles, drifting platforms, and a research vessel collected complementary in situ measurements (Fig. 3). This required considerable coordination to collate and assess the large amount of data collected each day, to review and update scientific and logistical objectives, and to pilot the many platforms to optimally achieve these objectives. The following subsections discuss the program design for the measurements, modeling, coordination, and data management.

a. Experimental design. The study region, about 100–300 km west of San Francisco, California, was chosen based on a balance of factors. Its regional dynamics, specifically

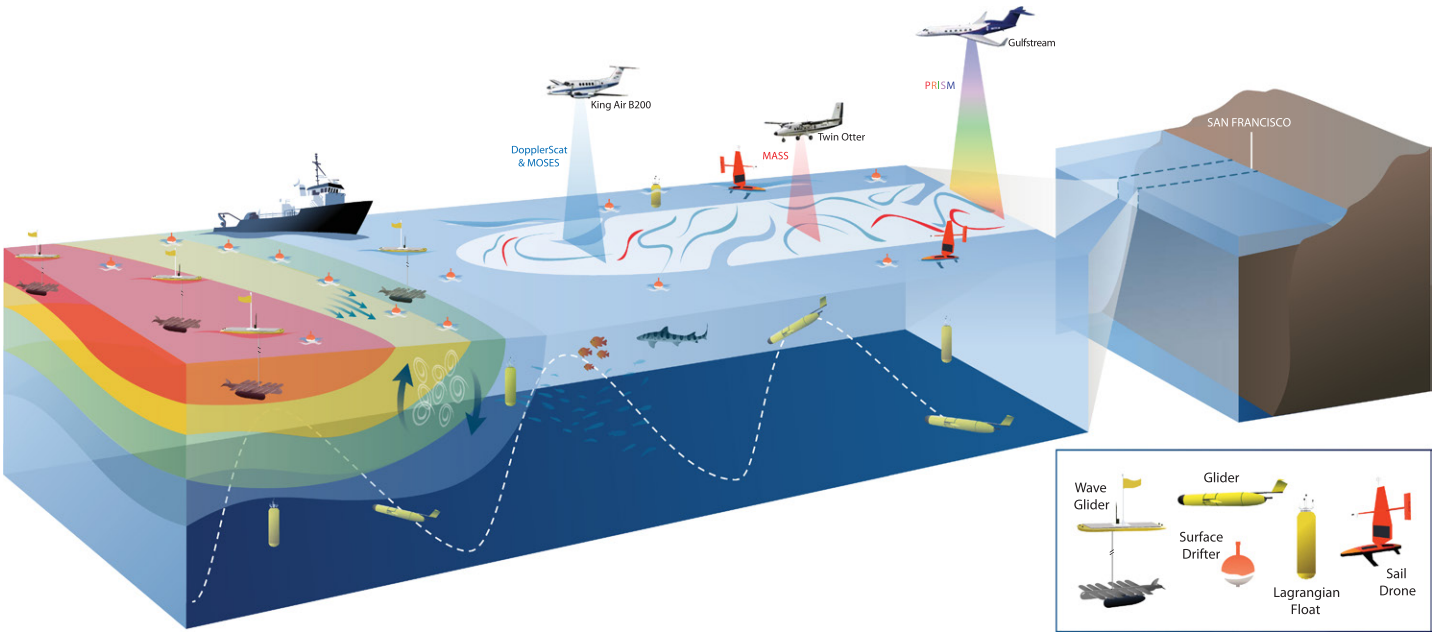

Fig. 3. Conceptual schematic of the S-MODE sampling strategy (from Farrar et al. 2020, illustration by Jennifer Matthews, SIO).

the presence of the California Current and seasonal upwelling, are favorable to the development of fronts and submesoscale instabilities, making it a focal point for previous modeling and observational studies of submesoscale dynamics (e.g., Capet et al. 2008a,b,c; Johnson et al. 2020). The region is also close to the NASA Ames Research Center and Moffett Field, which could be used as a base for aircraft operations. Most of the region just offshore of the California coast is classified as Special Use Airspace, meaning aircraft activities are subject to restrictions that could disrupt research flight operations, but there is an opening in the restricted areas near San Francisco that defines the northern, southern, and eastern boundaries of our study area (Fig. 4). The region also benefited from daily high-resolution sea surface topography imaging during the fast-repeat orbit of the Surface Water Ocean Topography (SWOT) satellite mission (Morrow et al. 2019; Fu et al. 2024).

S-MODE consisted of three separate field campaigns, a "pilot campaign" in October 2021 and two "intensive operations periods" (IOPs) in October 2022 and April 2023. The pilot campaign was a reduced-scale deployment to test ideas for the sampling strategy and to identify issues related to the interoperability of the many different platforms. The two IOPs took place in contrasting seasons: in spring (April 2023) when the ocean mixed layer was deep and in fall (October 2022) when the ocean mixed layer was shallow. We allowed a full year between the pilot campaign and the first IOP to fully learn lessons from the successes and failures of the pilot campaign. (Some lessons can only be learned by analyzing hard-won data to discover it would have been better to have done things differently.) The global COVID-19 pandemic disrupted a planned pilot campaign in April 2020, which was ultimately moved to October 2021. More details on the three campaigns are given in section 3.

b. In situ and airborne observations. Many different instrument platforms were operated together in a coordinated way to make sustained observations of ocean velocity, temperature, salinity, and bio-optical properties (Table 1). This section presents an overview of the observations made from the aircraft, ships, autonomous vehicles, and drifting platforms.

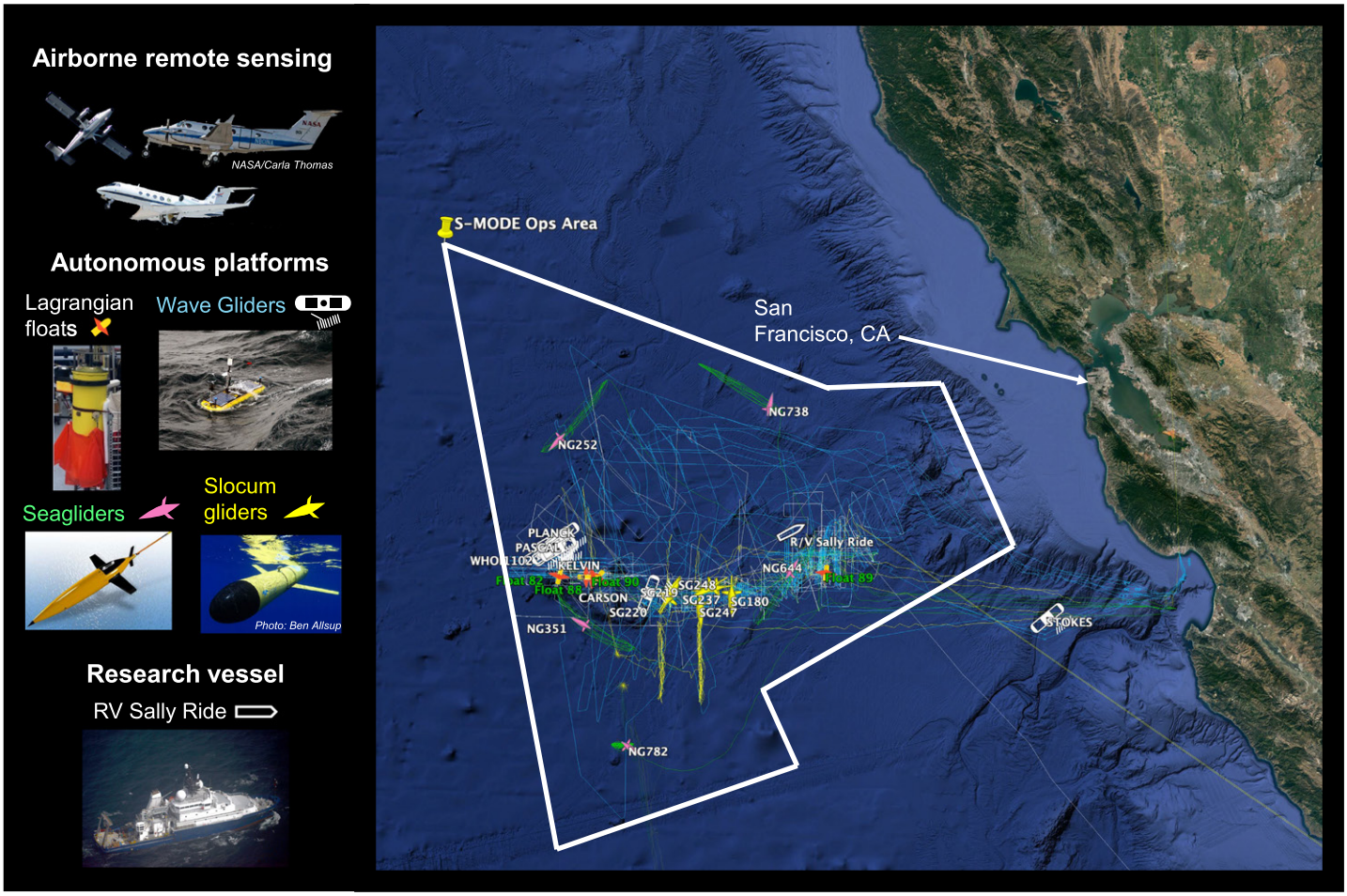

FIG. 4. **S-MODE operations area (white polygon) during the IOP2. (left) Photographs of the aircraft, autonomous platforms, and R/V *Sally Ride* used during IOP2. Colored tracks show the positions of different platforms. (top left) The three aircraft (Twin Otter, B200, and Gulfstream-III) carried instruments to measure ocean currents, surface winds, SST, waves, and ocean color, as described in section 2.**

1) AIRCRAFT REMOTE SENSING. S-MODE used three research aircraft: A NASA King Air B200 from the NASA Armstrong Flight Research Center carried the NASA/JPL DopplerScatt instrument and the University of California, Los Angeles (UCLA), Multiscale Observation System of the Ocean Surface (MOSES) instrument; a Twin Otter aircraft from Twin Otter International carried the Scripps MASS and DoppVis instruments; and a NASA Gulfstream III from Langley Research Center carried the Portable Remote Imaging Spectrometer (PRISM) hyperspectral radiometer.

(i) NASA/JPL DopplerScatt Doppler scatterometer. Circular scanning beam radar scatterometers, such as NASA's QuikSCAT satellite instrument, measure the radar backscatter from short ocean surface waves over multiple azimuth angles and a large swath. DopplerScatt is a Ka-band radar, measuring shorter waves (~0.5 cm) than QuikSCAT, which was a Ku-band radar measuring ~1-cm waves. By adding the capability to simultaneously measure the Doppler frequency shift of the radar backscatter, DopplerScatt (Rodríguez et al. 2018; Wineteer et al. 2020b; Rodríguez et al. 2020) provides estimates of the radial velocity of the short ocean waves. Using empirical geophysical model functions (GMFs), backscatter and radial velocity measurements are converted to estimates of 200-m resolution coincident vector winds and surface currents. The S-MODE campaigns provided a large number of independent surface current and wind measurements from Saildrones, Wave Gliders, surface drifters, and the DoppVis instrument (all described below) that helped to refine and validate

Table 1. Platforms, instruments, and variables measured during each campaign. Abbreviations: "IOP" = intensive operations period; "SST" = sea surface temperature; "SSS" = sea surface salinity; "CTD" = conductivity–temperature–depth (for measuring salinity, temperature, and depth); "ADCP" = acoustic Doppler current profiler (for ocean current profiles); "MVP" = Moving Vessel Profiler; "EcoCTD" is an underway shipboard profiler for measuring *T*, *S*, and bio-optical properties; "waves" indicates significant wave height; "wave spectra" indicates directional wave spectra; "meteorology" indicates wind speed/direction, air temperature, humidity, and barometric pressure. More information on the instruments is given in section 2.

Platform	Pilot	IOP1	IOP2	Instruments	Variables measured
King Air B200 (NASA Armstrong Flight Res. Ctr.)	14 flights	18 flights	22 flights	DopplerScatt, MOSES	Wind, surface currents, SST
Twin Otter (Twin Otter International)	10 flights	11 flights	12 flights	DoppVis, MASS	Wind, surface currents, SST, hyperspectral, wave spectra
Gulfstream III (NASA Langley Research Center)	—	8 flights	8 flights	PRISM	Hyperspectral
Ship	R/V *Oceanus*	M/V *Bold Horizon*	R/V *Sally Ride*	EcoCTD/MVP, CTD, ADCP, radiosondes, underway data	Meteorology, SST/SSS atm. profiles of *T* and humidity, velocity profiles, temperature/salinity, oxygen, chlorophyll, optical backscatter
Start date	19 Oct 2021	7 Oct 2022	9 Apr 2023		
End date	9 Nov 2021	2 Nov 2022	2 May 2023		
Saildrones	5	4	—	Meteorology, CTD, ADCP, bio-optics	Meteorology, waves, SST/SSS, velocity profiles, chlorophyll, optical backscatter
Wave gliders	3	8	9	Meteorology, CTD, ADCP, bio-optics	Meteorology, wave spectra, solar/infrared radiation, SST/SSS, chlorophyll, optical backscatter, velocity profiles
Seagliders	—	6	6	CTD, ADCP, bio-optics	Temperature/salinity, chlorophyll, optical backscatter, velocity profiles
Slocum gliders	10	10	5	CTD, bio-optics	Temperature/salinity
Lagrangian floats	—	3	4	CTD, ADCP	Lagrangian trajectories, temperature/salinity, and velocity profiles
Surface drifters	46	55	138	Drifting GPS buoy	Surface currents
APEX floats	—	—	10	CTD	Temperature/salinity

the GMFs developed prior to 2021. During the S-MODE IOP1 and IOP2 campaigns, DopplerScatt repeatedly collected data over multiple parallel lines ~125 km in length, separated by ~4 km, to image an area of roughly 100 km × 40 km over a period of ~4 h. This overlapped sampling made it possible to image each point on the surface from multiple azimuth directions, allowing reduced measurement noise and improved estimates of retrieved wind and current fields and derived vorticity and divergence.

(ii) UCLA MOSES infrared imager. The MOSES flew aboard the King Air B200 aircraft. It operates in the longwave infrared (LWIR) spectrum (9–12.5 μm) and features a FLIR LWIR camera A6750sc with a strained-layer superlattice, capturing images at 640 × 512 pixels, integrated with an accurate GPS-aided inertial measurement unit (GPS/IMU). The MOSES camera was angled 10° off nadir to align with the DopplerScatt system. It generated sea surface temperature (SST) maps from georectified LWIR images across a 5.4-km swath with ~10 m-resolution, refined by pathlength linear correction to reduce atmospheric humidity effects.

(iii) Scripps MASS and DoppVis instruments. The Modular Aerial Sensing System (MASS) is an airborne instrument package built around a high-resolution airborne topographic lidar collocated with video, infrared, and hyperspectral imaging systems (Melville et al. 2016; Lenain and Melville 2017; Lenain et al. 2019). The system is coupled with an accurate GPS/IMU, permitting airborne measurements of the sea surface displacement and temperature with swath widths of up to several kilometers and horizontal spatial resolution down to 0.2 m.

The MASS instrument was installed on a Twin Otter DHC-6 aircraft, operated by Twin Otter International (Grand Junction, Colorado), that was equipped with an additional fuel tank to extend the range of the aircraft to up to 8 h to maximize on-station survey time. The system was deployed during all three field programs (Table 1).

A new imaging sensor called "DoppVis" was added to the MASS for the S-MODE project to obtain coincident observations of surface currents alongside the MASS observations described above. The surface currents are inferred from optical observations of the spatiotemporal evolution of surface waves that measure the Doppler shift caused by underlying current (Lenain et al. 2023; Freilich et al. 2023).

(iv) JPL PRISM hyperspectral imager. PRISM is an imaging spectrometer that maps upwelling solar-reflected spectral radiance from 380 to 1050 nm at 3-nm spectral sampling, with high radiometric sensitivity to enable coastal aquatic and ocean color applications. For the S-MODE campaign, PRISM was installed on a NASA Gulfstream-III aircraft. PRISM had a spatial ground sampling of approximately 10 m and a spatial swath of 6 km. Each PRISM acquisition, or flight line, was a long strip of data following the flight track. By flying back and forth in adjacent paths, a large mosaic could be constructed. PRISM acquired 88 flight lines for each of the two IOPs, focusing on cloud-free days when the solar-reflected water signals could be observed. PRISM radiance data were radiometrically calibrated using a shipboard radiometer as an in situ reference (Bruegge et al. 2021). Atmospheric features determined the wavelength calibration (Thompson et al. 2024). The resulting radiance was used to estimate directional surface reflectance (Thompson et al. 2019), which was then glint corrected and assessed for chlorophyll content (O'Reilly and Werdell 2019) and particulate organic carbon (Stramski et al. 2008).

2) Shipboard observations. We used a ship in each of the three campaigns [Research Vessel (R/V) *Oceanus* in the 2021 pilot campaign, Motor Vessel (M/V) *Bold Horizon* in the 2022 IOP1, and R/V *Sally Ride* in the 2023 IOP2] to carry out three key tasks:

1) Conduct rapid, multiscale hydrographic surveys of the upper ocean using shipboard instrumentation and towed conductivity–temperature–depth (CTD) profilers [either an EcoCTD as described by Dever et al. (2020) or an AML Oceanographic Moving Vessel Profiler (MVP)].
2) Deploy, service, recover, and reposition various autonomous instruments.
3) Provide a platform for biogeochemical, optical, and meteorological observations that could not be collected autonomously or remotely.

To balance these diverse and often conflicting objectives, shipboard operations alternated between different modes. For example, the ship would first perform a broad survey of the study area to identify and characterize submesoscale features for targeted investigation. Once a promising feature was identified, the ship would deploy autonomous drifting assets (such as Lagrangian floats and drifters) within it. The ship would then closely follow these drifting instruments, conducting detailed surveys to track the feature's evolution. These submesoscale features typically lasted only a few days before losing coherence and breaking apart. When that occurred, Lagrangian floats were retrieved, and the search for a new feature began. Surface drifters were left behind to provide context on the broader circulation patterns.

Shipboard water sampling, using both flow-through and CTD Rosette samplers, enabled calibration of the bio-optical tracer observations as well as characterization of nutrient distributions and community composition. Shipboard operations were tightly coordinated with autonomous instruments, satellite data, and aircraft overflights, enabling real-time decision-making to adapt to rapidly evolving conditions.

3) Autonomous vehicle observations.

(i) Underwater gliders. Underwater gliders are buoyancy-driven platforms that can steer through the water by controlling attitude (pitch and roll) and can thus navigate between waypoints to execute survey patterns. Two types of underwater gliders were used in S-MODE: Seagliders, built and operated by a team from the Applied Physics Laboratory at the University of Washington, and Teledyne Webb Slocum Gliders, operated by a team from the U.S. Naval Oceanographic Office (NAVO) and Naval Research Laboratory (NRL).

The UW-APL Seagliders were piloted along repeated lines to measure the temporal evolution of the upper ocean at scales of 2–50 km and to 1000-m depth. The gliders carried CTDs, oxygen optodes, bio-optical instruments (WetLabs ECO Pucks to measure chlorophyll fluorescence and optical backscatter), and acoustic Doppler current profilers (ADCPs) to estimate the currents.

NAVO gliders focused on measuring the ocean mesoscale structure. The primary instruments of the NAVO gliders were CTDs, but they also carried measured optical backscatter during the pilot campaign and IOP1. During IOP1, the NAVO gliders were piloted by an automated system that was designed to reduce the forecast errors in the NRL Navy Coastal Ocean Model forecast system by directing the gliders to move toward regions with high forecast uncertainty.

(ii) Uncrewed surface vehicles. A fleet of 8–12 uncrewed surface vehicles (USVs) were operated in formation during each of the campaigns to measure subsurface vertical profiles of velocity and the horizontal velocity gradients. There were two kinds of USVs: Wave Gliders (Hodges et al. 2023; Grare et al. 2021) and Saildrones (Gentemann et al. 2020; Stevens et al. 2021).

Five Saildrones were deployed in the pilot campaign and four Saildrones were deployed in IOP1, together collecting 41 days of data from the two field campaigns. The Saildrones were equipped with over 10 scientific sensors (Table 1) to make measurements of the near-surface ocean and atmosphere, including a Teledyne RD Instruments Workhorse 300-kHz ADCP. The main mode of sampling was sailing in kilometer-scale formations to map horizontal density gradients, velocity gradients, and derived kinematic properties across different submesoscale features. We typically tried to arrange the Saildrones into a 2-km square or a quincunx (like the five on playing dice), maintaining the formation as they moved. We also operated Saildrones in other sampling modes to optimize their value in the experiment. At the beginning of each campaign, Saildrones, in conjunction with other platforms, performed mesoscale surveys to help determine potential features of interest for intensive submesoscale sampling. During the pilot campaign, Saildrones sampled parallel tracks within <2 km of R/V *Oceanus* and other assets for velocity intercomparisons. At the end of IOP1, Saildrones spread out in four parallel tracks separated by 10 km to map the horizontal structure of mature submesoscale instabilities that developed downstream of a strong front.

The Wave Gliders, equipped as described in Hodges et al. (2023), all carried instruments for measuring ocean current profiles from 4- to 100-m depth (300-kHz Teledyne RD Instruments Workhorse ADCPs), ocean temperature and salinity at multiple depths (Seabird Glider Payload CTDs and RBR*concerto*^{3} CTDs), ocean wave directional spectra (using dual-GPS/inertial measurement units), vector winds, precipitation, air temperature, and humidity. Some of the Wave Gliders also carried additional ADCPs (Nortek Signature 1000) to obtain better resolution of the current profiles near the surface, radiometers to measure downward solar and infrared radiation, and instruments to measure ocean bio-optical properties. In IOP2, one of the Wave Gliders ("Carson") also measured CTD profiles with a winched profiler that made measurements from 10- to 100-m depth. The Wave Gliders were spread out to survey a large area at the beginning of each campaign to help identify features of interest, and they were brought into kilometer-scale arrays after features of interest were identified.

4) Drifting platform observations.

(i) Surface drifters. A total of 237 satellite-tracked surface drifters were deployed across the three campaigns to measure near-surface currents over a wide range of space and time scales. The mix of CARTHE (Novelli et al. 2017) and Microstar drifter designs measured currents centered at 0.3- and 1.0-m depth, respectively. The experimental area was densely populated with surface drifters to enable long-term tracking of submesoscale features and to capture circulation patterns across multiple scales.

Drifter deployment tactics varied based on the experimental needs. During the initial survey of each submesoscale feature, a line of 4–10 drifters, spaced 1–2 km apart, was typically deployed across the feature. These drifters provided real-time information on the evolution of the feature, guiding subsequent surveys. A drifter was also deployed with each Lagrangian float to assist in tracking the float while it was submerged. Convergence of surface drifters helped to identify and track fronts and eddies where the drifters tend to accumulate (D'Asaro et al. 2018). Drifters typically remained within the S-MODE sampling area for 5–10 days, and we deployed more as needed to inform sampling by other platforms.

(ii) Lagrangian floats. Lagrangian floats, which can follow the 3D motion of the water (D'Asaro 2003), measured vertical velocity, vertical shear, stratification, oxygen, optical backscatter, and chlorophyll in submesoscale fronts and eddies in both IOPs. Vertical velocity was measured both from the vertical motion of the float when operated in a water-following mode and from the upward beam of a Signature1000 ADCP (Shcherbina et al. 2018). The floats were deployed in kilometer-scale arrays in or near the target features and were operated either within the mixed layer, following the turbulent water trajectories, or just below it to measure the vertical velocity across the mixed layer with the ADCP.

(iii) APEX floats. During IOP2, NAVO also deployed 10 APEX floats that carried CTDs. These floats are physically identical to APEX floats used in the global Argo program. They do not follow the water as the Lagrangian floats do; instead, they profile vertically from the surface to 1000-m depth. The floats were spread around the S-MODE sampling domain to measure the evolution of temperature, salinity, and density on larger (100 km) scales.

c. Ocean modeling. Most of our understanding of submesocale dynamics comes from models, and a major motivation for S-MODE is to determine what is and is not realistic in these models. Thus, modeling is an integral component of S-MODE. The modeling methodologies are of three types: (i) regional forward modeling (using observed forcing fields but unobserved boundary and initial conditions taken from larger-scale simulations); (ii) forecast (runs going several days into the future with observed forcing and observed initial conditions, usually inherited from large-scale measurements); and (iii) reanalysis (incorporating the available observations in post hoc forecasts).

1) Forward modeling. The rationale for forward modeling is that the intrinsic variability of oceanic eddies can most realistically be represented by free-running, quasi-equilibrium simulations without any interior disruption of the dynamical equations, while evolving under the external influences of specified surface meteorological and tidal gravitational forcing and open boundary conditions obtained from a larger-scale model run on a coarser grid with analogous forcing.

Two high-resolution forward model simulations were used in S-MODE to depict eddy patterns, statistics, and processes in ways that can be compared to the measurements. The Regional Oceanic Modeling System (ROMS) simulation from the UCLA group (Fig. 2, left) is for a nested subdomain in a full Pacific simulation. The simulation has realistic high-frequency

wind and tidal forcing, and the inner domain has a horizontal grid resolution of 200 m. The MITgcm (Marshall et al. 2004) simulation from NASA-JPL/Caltech group (Fig. 2, right) is also for a nested subdomain with realistic high-frequency wind and tidal forcing and an inner grid resolution of 500 m (Torres et al. 2022).

2) Reanalysis and forecasting. During each of the three S-MODE campaigns, the NRL produced real-time ocean model forecasts covering the geographic regions of interest. Model forecasts were created using the Navy Coastal Ocean Model (NCOM) (e.g., Yu et al. 2023) with a horizontal resolution of 1 km and 100 vertical layers. Model forecast fields were corrected daily via three-dimensional variational data assimilation (3DVAR) using the Navy Coupled Ocean Data Assimilation (NCODA) (e.g., Jacobs et al. 2014) system. All of the regularly available observations were assimilated (i.e., nadir altimetry, satellite SST, and Argo floats) as well as data from the Slocum gliders (NAVO), APEX floats (NAVO), and the Seagliders (UW-APL). During the pilot campaign and IOP-2, model adjustments with NCODA used assimilation scales based on the local Rossby radius of deformation. During IOP1, a novel data assimilation approach was employed, whereby the assimilation scales were a function of the local observation density, making corrections at smaller scales where high-resolution in situ data were available. The method produced lower model errors in the S-MODE region (Jacobs et al. 2023). Each day during the campaigns, data assimilation state estimates and 96-h forecast fields were provided to the S-MODE team.

d. The S-MODE "control center". S-MODE required the coordination of a large number of platforms in response to rapidly changing oceanographic conditions. Traditionally, decision-making for adaptive sampling in oceanographic field campaigns has been made on a ship. However, the need to coordinate a large number of observing platforms led the S-MODE team to form a dedicated control center onshore, with the ship being one important platform among many. The control center was originally planned to be located at the NASA Ames Research Center, tied to the need for daily aircraft flight plans and briefings, but the COVID-19 pandemic drove us to have a virtual control center, which turned out to have advantages we did not anticipate.

The central elements of the control center were a data system, dedicated analysis scientists, participation by all platform operators, and advice from other team members. A dedicated website gathered all relevant data from platforms and models and allowed the real-time display of critical information, most importantly the location of all platforms. The data system was planned and developed months in advance, tested during the pilot campaign, and operated continuously during each of the field campaigns. The analysis of the large volumes of daily data was spread across the team, with many analyses automated and integrated into the data system as lessons were learned. Information and updates were shared with the whole team using a messaging app (Slack). The effort was operated on a daily schedule of briefings, conducted by the chief mission scientist, first with the platform operators and a few hours later with the entire science team, with a goal of defining the overall sampling plan for the next day by the late afternoon. The briefings were typically attended by about 40 people, all remotely, plus most of the science party on the ship. Briefings included an operational update, an analysis of meteorological and oceanic conditions, and a proposed sampling plan, followed by discussion and modification of the plan. The detailed implementation of the plan as well as cross-platform coordination was determined by each of the platform teams.

The concept of a virtual control center not based at sea is relatively new to oceanography. It has the advantages of including a large and dispersed team in the decision-making process, including many early career scientists and scientists who could not go to sea because of other obligations. Without the need for travel or full-time commitment, a larger number

of interested experts could provide a valuable input. Graduate and undergraduate students participated in briefings to observe the real-time unfolding of a large field experiment. The main reason for the success of the approach was the nearly full-time commitment by the dispersed team to analyze the incoming data to guide the operations. The team was larger than could fit on a research vessel, was not subject to the difficulties of working at sea, and could therefore do more. As uncrewed, remotely piloted platforms make up increasingly large parts of oceanographic field campaigns, this concept of a decentralized virtual control center could prove increasingly important.

e. Data management. S-MODE investigators generated a diverse dataset that required careful curation to ensure that it can be fully utilized by the broader research community. S-MODE included a dedicated data management effort, with strict attention to standard protocols such as the NetCDF Climate and Forecast (CF) metadata convention (Eaton et al. 2022) and the Attribute Convention for Data Discovery (Earth Science Information Partners 2022) with standardized metadata. A NASA-mandated "Data Management Plan," submitted prior to the start of the investigation, described the instruments, quality control procedures, sampling protocols, data volumes, etc.

Data were submitted to the NASA Physical Oceanography Distributed Active Archive Center (PO.DAAC) by uploading to the cloud-based Amazon Simple Storage Service (also known as S3). The data were checked for compliance to the abovementioned conventions and then posted to a permanent archive with Digital Object Identifier (DOI)'s (Table 2) and dataset landing pages. The landing pages include links to technical reports and other documentation. More detail about the datasets is available in a technical report (Westbrook et al. 2024).

3. The S-MODE campaigns

a. Pilot campaign: October 2021. The pilot field campaign was conducted in fall 2021. Compared to IOP1 and IOP2, it used a reduced complement of platforms including the NASA B200 (DopplerScatt, MOSES), the Twin Otter aircraft (MASS/DoppVis), the R/V *Oceanus* (19 October–9 November), surface drifters, Saildrones, Wave Gliders, and NAVO Slocum gliders (Table 1). Sampling was focused on two oceanographic target regions (Fig. 5):

1) Around 25 October 2021, we sampled a strong SST front near 37°N, 125°W (Fig. 5). This front was sampled by DopplerScatt, MOSES, MASS/DoppVis, the R/V *Oceanus*, and five Saildrones (black dots in Fig. 5a). Over the course of a few days, we observed a rapid sharpening of the front (frontogenesis) and its collapse. An example of data from the MOSES infrared imager is shown in Fig. 5b.
2) From 2 to 5 November 2021, in the final days of the pilot campaign, we collected simultaneous measurements from the B200, Twin Otter, Wave Gliders, Saildrones, ship, drifters, and coastal HF radar (part of the Southern California Coastal Observing System; Harlan et al. 2010) within a region where strong and weak velocity gradients occurred in close proximity (Fig. 5c). Nicknamed as the "velocity extravaganza," this activity focused on intercomparison of ocean current observations.

Weather conditions were challenging during the beginning of the pilot field campaign. An extratropical cyclone developed over the Northwest Pacific and rapidly intensified into a bomb cyclone as it moved eastward across the North Pacific. This system led to a category 5 atmospheric river event on 24 October, causing extreme sea states (>10-m waves). Two of the Wave Gliders were damaged by a rogue wave that washed over the back of the R/V *Oceanus*. The extreme sea state also led to a mechanical failure of the *Oceanus*' controllable pitch propeller on 22 October 2021, just as it was arriving at the S-MODE operation area to begin

TABLE 2. **Available S-MODE datasets with associated DOIs. The check marks indicate campaigns in which a given platform was deployed (with the exception of the L3 Shipboard UCTD and EcoCTD, which has only been produced for one campaign).**

Dataset	DOI	PFC	IOP1	IOP2
Aircraft data				
S-MODE L1 MASS DoppVis imagery version	https://doi.org/10.5067/SMODE-MASS1D	✓	✓	✓
S-MODE L1 MASS hyperspectral imagery	https://doi.org/10.5067/SMODE-MASS1H	✓	✓	✓
S-MODE L1 MASS Lwir	https://doi.org/10.5067/SMODE-MASS1I	✓	✓	✓
S-MODE L1 MASS lidar point cloud	https://doi.org/10.5067/SMODE-MASS1L	✓	✓	✓
S-MODE L1 MASS visible imagery	https://doi.org/10.5067/SMODE-MASS1V	✓	✓	✓
S-MODE L1 PRISM	https://doi.org/10.5067/SMODE-PRSM1	—	✓	✓
S-MODE L2 PRISM chlorophyll-a	https://doi.org/10.5067/SMODE-PRSM2-CHLA	—	✓	✓
S-MODE L2 PRISM reflectance	https://doi.org/10.5067/SMODE-PRSM2-REFL	—	✓	✓
S-MODE L2 MOSES	https://doi.org/10.5067/SMODE-MOSE2	✓	✓	✓
S-MODE L1 DopplerScatt	https://doi.org/10.5067/SMODE-DSCT1	✓	✓	✓
S-MODE L2 DopplerScatt	https://doi.org/10.5067/SMODE-DSCT2	✓	✓	✓
In situ data				
S-MODE L2 shipboard CTD	https://doi.org/10.5067/SMODE-RVCTD	✓	✓	✓
S-MODE L2 shipboard ADCP	https://doi.org/10.5067/SMODE-RVADC	✓	✓	✓
S-MODE L2 shipboard TSG/MET	https://doi.org/10.5067/SMODE-RVTSG	✓	✓	✓
S-MODE L2 shipboard uCTD and EcoCTD	https://doi.org/10.5067/SMODE-RVECT	✓	✓	✓
S-MODE L3 shipboard uCTD and EcoCTD	https://doi.org/10.5067/SMODE-RVECT3	✓	—	—
S-MODE L2 shipboard bottle data	https://doi.org/10.5067/SMODE-RVBOT	✓	✓	✓
S-MODE L2 shipboard SUNA	https://doi.org/10.5067/SMODE-RVSUN	✓	—	—
S-MODE L2 shipboard radiometer	https://doi.org/10.5067/SMODE-RVRAD	✓	✓	✓
S-MODE L2 Wave Glider observations	https://doi.org/10.5067/SMODE-WAVGL2	✓	✓	✓
S-MODE L2 surface drifter positions	https://doi.org/10.5067/SMODE-DRIFT	✓	✓	✓
S-MODE L2 Saildrone data	https://doi.org/10.5067/SMODE-SDRON	✓	✓	
S-MODE L2 radiosonde data	https://doi.org/10.5067/SMODE-SONDE	✓	✓	✓
S-MODE L2 Slocum glider data	https://doi.org/10.5067/SMODE-GLID2	✓	✓	✓
S-MODE L2 Lagrangian float data	https://doi.org/10.5067/SMODE-FLOAT	—	✓	✓
S-MODE L2 Seaglider data	https://doi.org/10.5067/SMODE-SEAGL2	—	✓	✓
S-MODE L2 NAVO float data	https://doi.org/10.5067/SMODE-APEX2	—	—	✓
Model data				
S-MODE L4 NCOM	https://doi.org/10.5067/SMODE-NCOM	✓	✓	✓
S-MODE L4 ROMS	https://doi.org/10.5067/SMODE-ROMS	—	—	✓

collecting data. The ship made a short port call in San Francisco from 24 to 27 October 2021 to make repairs to the ship and the Wave Gliders.

b. IOP1: October 2022. IOP1 took place in fall 2022. It consisted of a 26-day cruise on the M/V *Bold Horizon* (7 October–2 November 2022) and deployments of Saildrones, Wave Gliders, Seagliders, Slocum gliders, Lagrangian floats, surface drifters, the Gulfstream-III (PRISM), the King Air B200 (DopplerScatt, MOSES), and the Twin Otter (MASS/DoppVis).

After surveying the area, the observations focused on an oceanic front as it steepened and developed instabilities (Fig. 6, near 37°N, 124.5°W). We obtained persistent measurements of this front for the duration of the campaign. There were two contrasting weather regimes in IOP1: one with weak winds, thick low clouds, occasional fog, and higher relative humidity (1–18 October 2022) and a second regime with stronger winds, partly cloudy skies, large

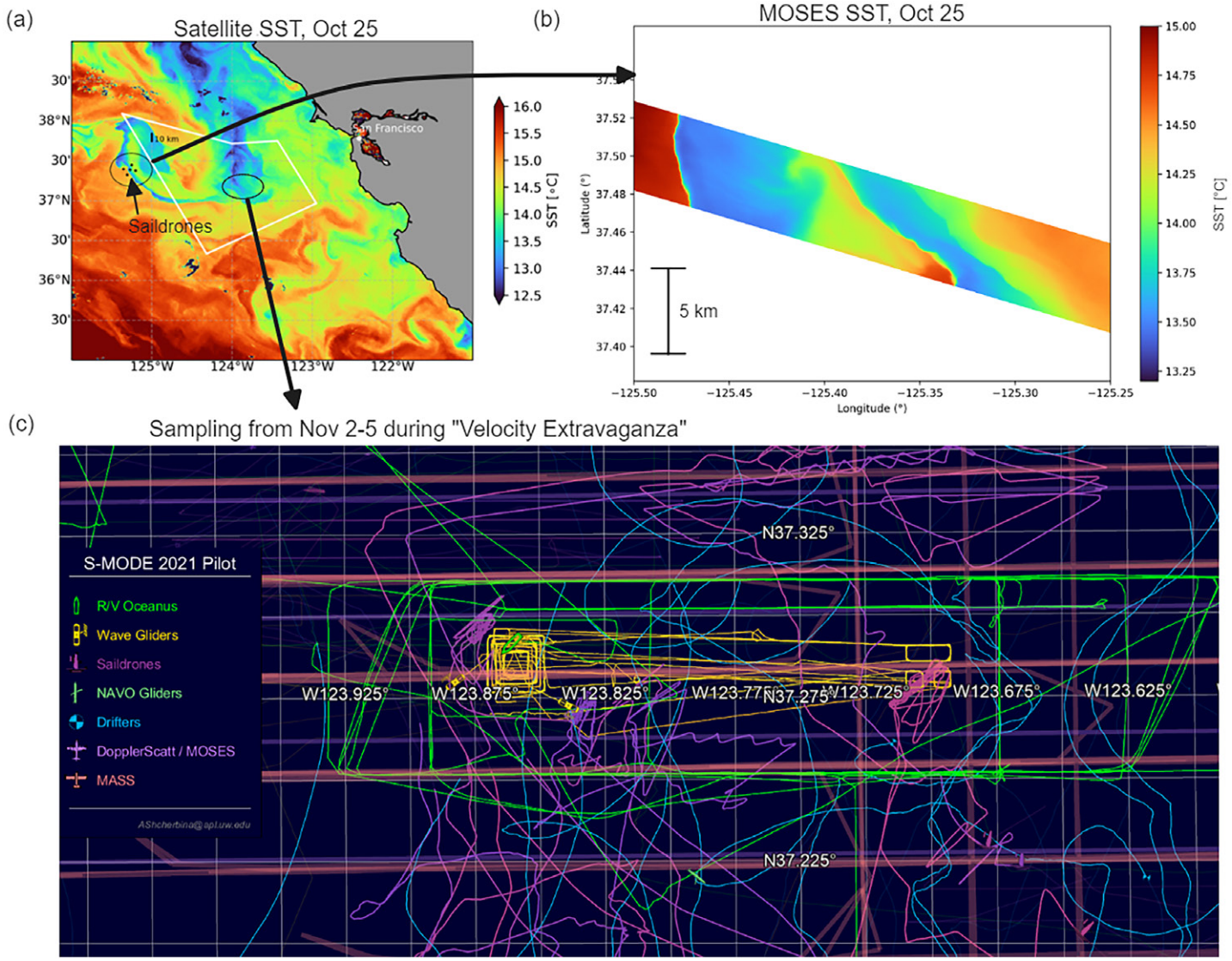

FIG. 5. (a) SST from the Visible Infrared Imaging Radiometer Suite (VIIRS) instrument on the *Suomi NPP* satellite during the pilot campaign (25 Oct 2021). (left circled region) The first oceanographic target , and the black dots indicate the positions of the Saildrones around the time of the satellite overpass and the aircraft sampling. (b) High-resolution SST measured from the MOSES instrument on the same day from the NASA B200 aircraft showing a very sharp front near 125.47°W and development of submesoscale eddies near 37.5°N, 125.4°W and 37.45°N, 125.35°W. (c) Sampling during the pilot campaign velocity extravaganza activity on 2–5 Nov when the team conducted an intensive period of ocean current velocity intercomparisons between different instruments.

waves, and lower relative humidity (19–30 October 2022). The long period of cloudiness reduced the effectiveness of the solar panels on the Saildrones and Wave Gliders, forcing us to turn off some instruments to save power and causing some data gaps.

c. IOP2: April 2023. IOP2 was conducted in the spring of 2023, with a 26-day cruise on the R/V *Sally Ride* (9 April–2 May 2023), and deployments of Wave Gliders, Seagliders, Slocum gliders, 138 surface drifters, APEX floats, Lagrangian Floats, the NASA Gulfstream-III (PRISM), the NASA B200 (DopplerScatt and MOSES), and the Twin Otter (MASS/DoppVis). Importantly, IOP2 overlapped with the special Fast Sampling Phase of the SWOT satellite (Morrow et al. 2019), and much of the S-MODE data from IOP2 are coincident with SWOT data.

A series of atmospheric river events from December 2022 to March 2023 caused heavy rainfall over California, unusually high river discharge, and fresh, high-chlorophyll water near the coast. In April 2023, there was a plume of cool, fresh, high-chlorophyll water that was being advected

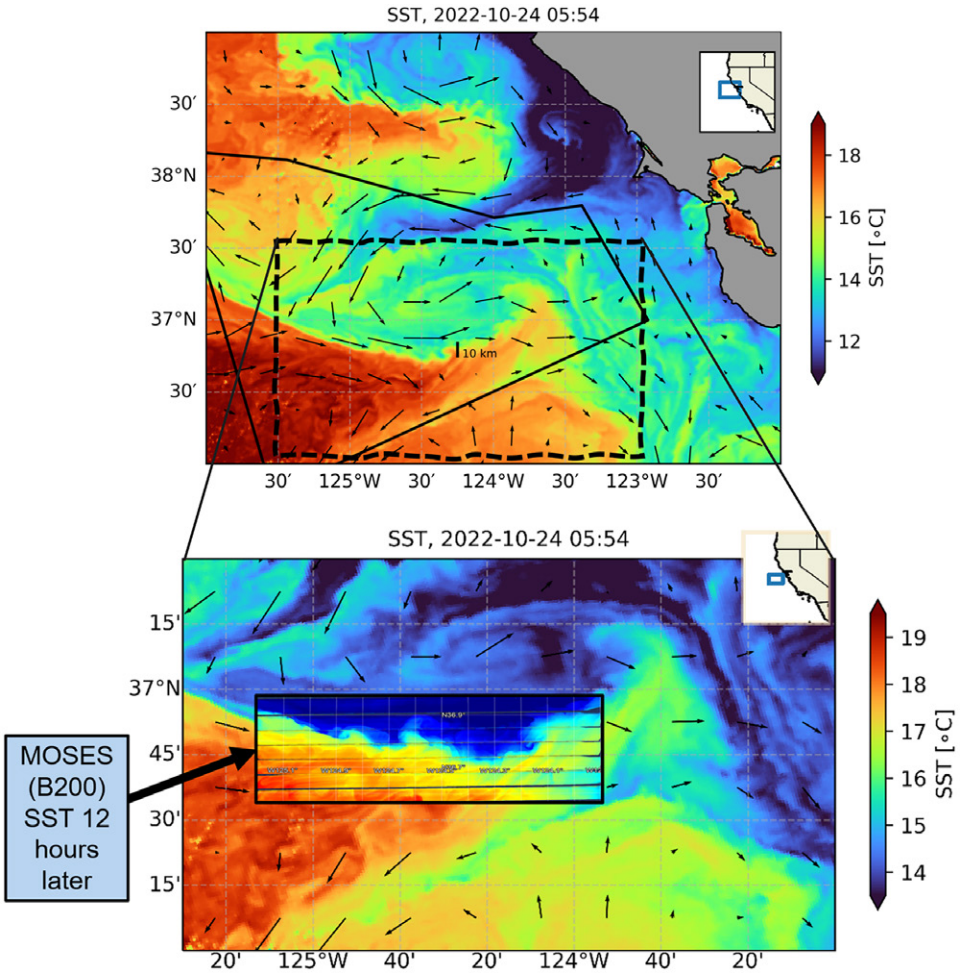

Fig. 6. (upper) SST during IOP1 on 24 Oct 2022 (from the *Sentinel 3A* satellite), with ocean current vectors estimated from the Copernicus Marine and Environment Monitoring Service (CMEMS) gridded-altimetry product (Pujol et al. 2016; CMEMS 2023). Numerous submesoscale fronts and instabilities can be seen at scales less than 10 km (see scale bar near middle of panel). (lower) A higher resolution view of the SST under the flight path of the NASA B200 aircraft taken with the MOSES infrared imager about 12 h later. (An even higher resolution view is shown in Fig. 10.)

offshore by the mesoscale current field (Fig. 7; also see Fig. 4). The plume was almost continuously developing submesoscale instabilities; the sampling was focused primarily on the "upstream" region of the plume, and the ship, Wave Gliders, and Lagrangian platforms stayed with one of the developing eddies as it intensified and moved westward in the plume. We saw various weather patterns over the course of IOP2, including periods of weak winds and a multiday period with stronger winds and atmospheric boundary layer roll vortices.

4. Discussion and conclusions: Toward meeting the scientific goals of S-MODE

To test the hypothesis that submesoscale ocean dynamics make important contributions to vertical exchange in the upper ocean, the S-MODE science team set four science goals:

1) Quantitatively measure the three-dimensional structure of the submesoscale features responsible for vertical exchange.
2) Examine vertical transport processes at submesoscales to mesoscales.
3) Understand the relation between the velocity (and other surface properties) measured by remote sensing at the surface and that within the ocean surface boundary layer.
4) Quantify the role of air–sea interaction and surface forcing in the dynamics and vertical velocity of submesoscale variability.

The bulk of this paper has described our approach to meeting the first goal. The last three goals pose more difficult challenges.

Measurement of vertical velocity (goal 2) is a notoriously difficult task because measurements of vertical velocity are easily swamped by relatively small errors in the much larger horizontal velocity. The dense measurements of horizontal velocity made from aircraft remote sensing and from arrays of in situ platforms enable a relatively new approach to estimate vertical velocity by estimating horizontal divergence at kilometer scales to infer vertical velocity at those scales (see Rudnick et al. 2022, for an example from another experiment). Already proven techniques for measurements of vertical velocity from Lagrangian floats and from horizontal divergence estimates from surface drifters (e.g., D'Asaro et al. 2018; Tarry et al. 2021) give us a means to validate the newer estimates based on horizontal divergence estimated from remote sensing and arrays of autonomous platforms.

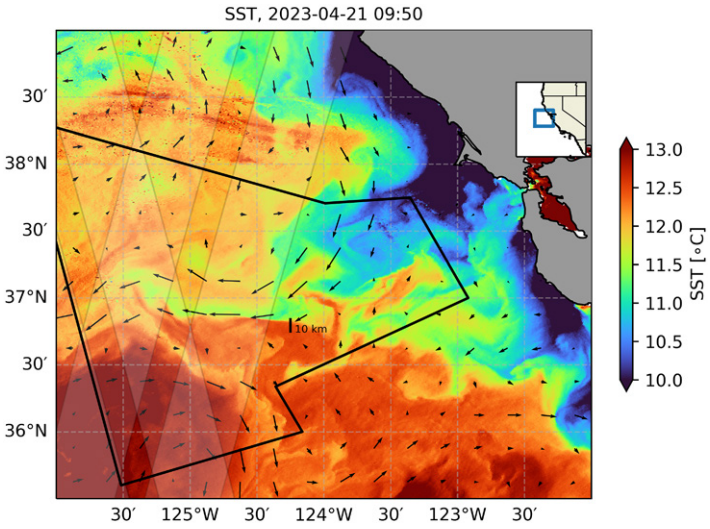

FIG. 7. SST during IOP2 on 21 Apr 2023 (from the VIIRS instrument on the *NOAA-20* satellite). Sampling was concentrated on instabilities forming along a plume of cool, fresh, high-chlorophyll water that was being pulled offshore by the lager mesoscale current field. The black vectors are estimates of the mesoscale geostrophic velocity field from the CMEMS gridded-altimetry product (Pujol et al. 2016; CMEMS 2023, accessed on 15 May 2023), and the faint white swaths show the sampling of the SWOT satellite during its Fast Sampling Phase.

The size of submesoscale horizontal divergence variations is expected to be comparable to the size of the Coriolis parameter f which is about 9×10^{-5} s^{-1} at the latitude of S-MODE. Standard propagation of errors suggests that measuring the horizontal velocity gradient with an accuracy of $0.15f$ at 1-km separation would require a velocity accuracy of 1 cm s^{-1}, which is at the edge of present observational capabilities. Understanding and reducing measurement errors for ocean velocity has thus been a major focus of S-MODE (e.g., Rodríguez et al. 2020; Hodges et al. 2023).

Understanding the relation between remotely sensed surface properties and in situ properties of the ocean surface boundary layer (goal 3) is critical for interpreting the aircraft-derived synoptic maps obtained during S-MODE. For example, inference of vertical velocity from DopplerScatt surface current divergence requires knowledge of the vertical structure of near-surface currents; there has been some progress here (Samelson 2022; Lenain et al. 2023), but there is more to do. S-MODE used multiple platforms to observe multiple quantities simultaneously. One example is shown in Fig. 8, which illustrates the rich and complex relationship between surface currents (DoppVis), SST (MASS), and surface chlorophyll-a (PRISM) on 19 April 2023 (IOP2). A submesoscale cyclone is visible in the center of the upper panels, where the velocity field is swirling counterclockwise and the SST field is wrapping into a spiral around a cooler eddy core with high chlorophyll. The lower panels illustrate the rich detail that is present at even finer scales.

The in situ data help to reveal the subsurface structures associated with these surface signals. The submesoscale eddy seen in Fig. 8 was sampled by R/V *Sally Ride* for about 2 weeks. Six days after the MASS and DoppVis flights (Fig. 8), the research vessel made transects through the center of the submesoscale cyclone to record high-resolution vertical

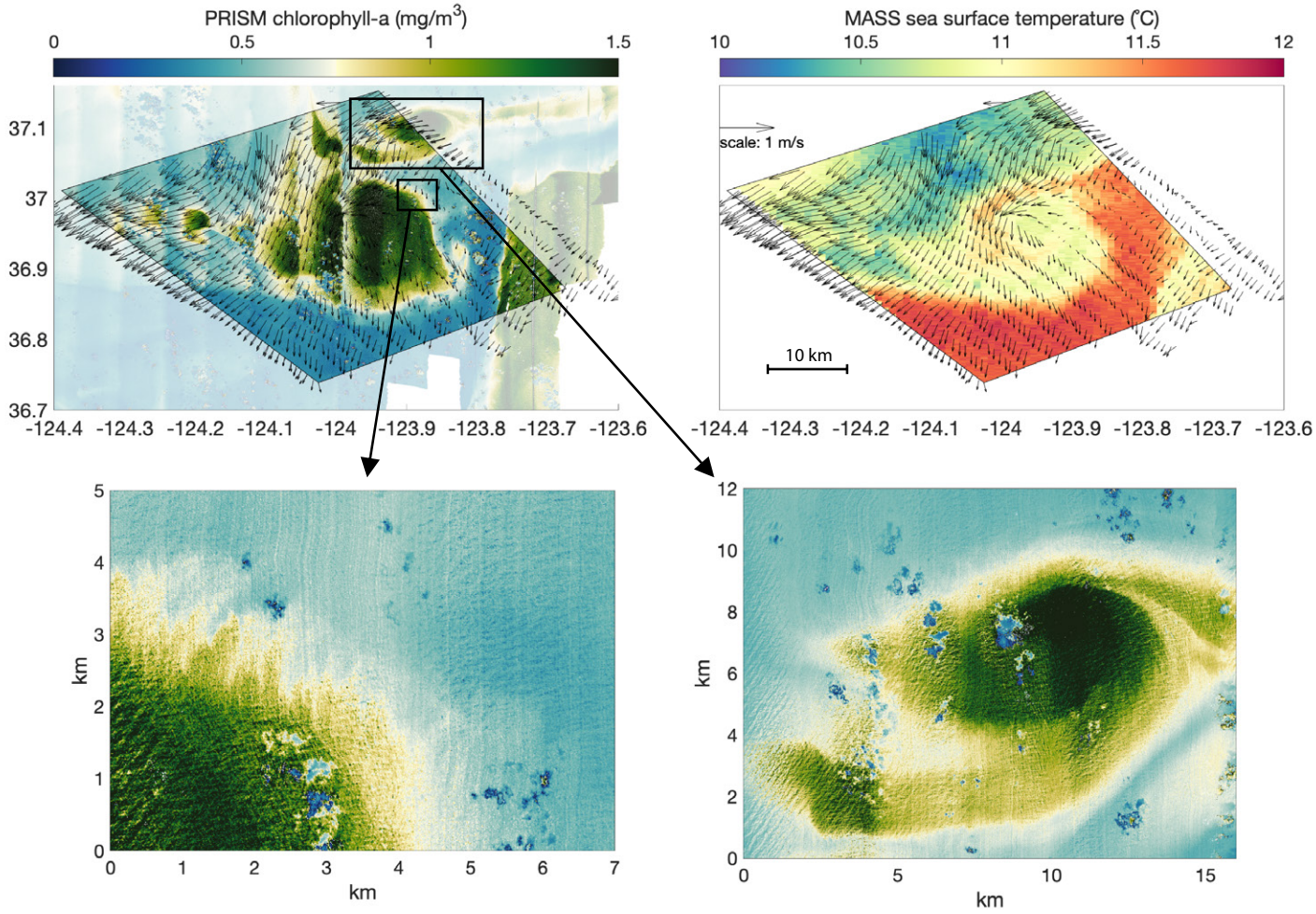

FIG. 8. Observations on 19 Apr 2023 (IOP2) of a submesoscale ocean cyclone seen in (top left) chlorophyll-a (PRISM) and (top right) SST (MASS) with overlain surface currents (DoppVis; black vectors). (bottom left–right) Zoomed-in views of PRISM chlorophyll-a of (left) the northeastern edge of the submesoscale cyclone and (right) a nearby smaller submesoscale feature. (top left) The chlorophyll-a data show some banding due to sunglint, caused by mosaicking adjacent flight lines with wide (±15°) fields of view. Refinements to glint models are ongoing for future versions of the data.

profiles of ocean salinity, temperature, and chlorophyll, and DopplerScatt flights provided high-resolution fields of surface vorticity and winds (Fig. 9). With its comprehensive surface and subsurface data, S-MODE will be able to relate high-resolution surface measurements to the vertical structure of the properties within and below the surface boundary layer to examine vertical exchange processes at submesoscales. The data also present valuable opportunities to compare observations with numerical models, a major goal of S-MODE.

S-MODE has also provided unique measurements that address how air–sea interaction and surface forcing both modulate and respond to submesoscale variability (goal 4). Figure 10 illustrates the combined synoptic observations of SST, currents, and winds obtained on 24 October 2022 with the MOSES and DopplerScatt instruments, showing a more detailed view of the scene already shown in Fig. 6. The surface current streamlines have a close relationship to the SST field observed simultaneously by the MOSES infrared imager (Fig. 10a). The vorticity field (Fig. 10b) reveals a cyclonic eddy near the center of the image (near $x = -7$ km, $y = 7$ km), and the simultaneous wind speed measurements from DopplerScatt show a striking modulation of wind speed as the wind blows from north to south across the oceanic front. This is an exciting new view of ocean dynamics and air–sea interaction, and we are pleased to have captured many different scenes like this one under varying conditions during the three campaigns. The S-MODE team is eagerly analyzing

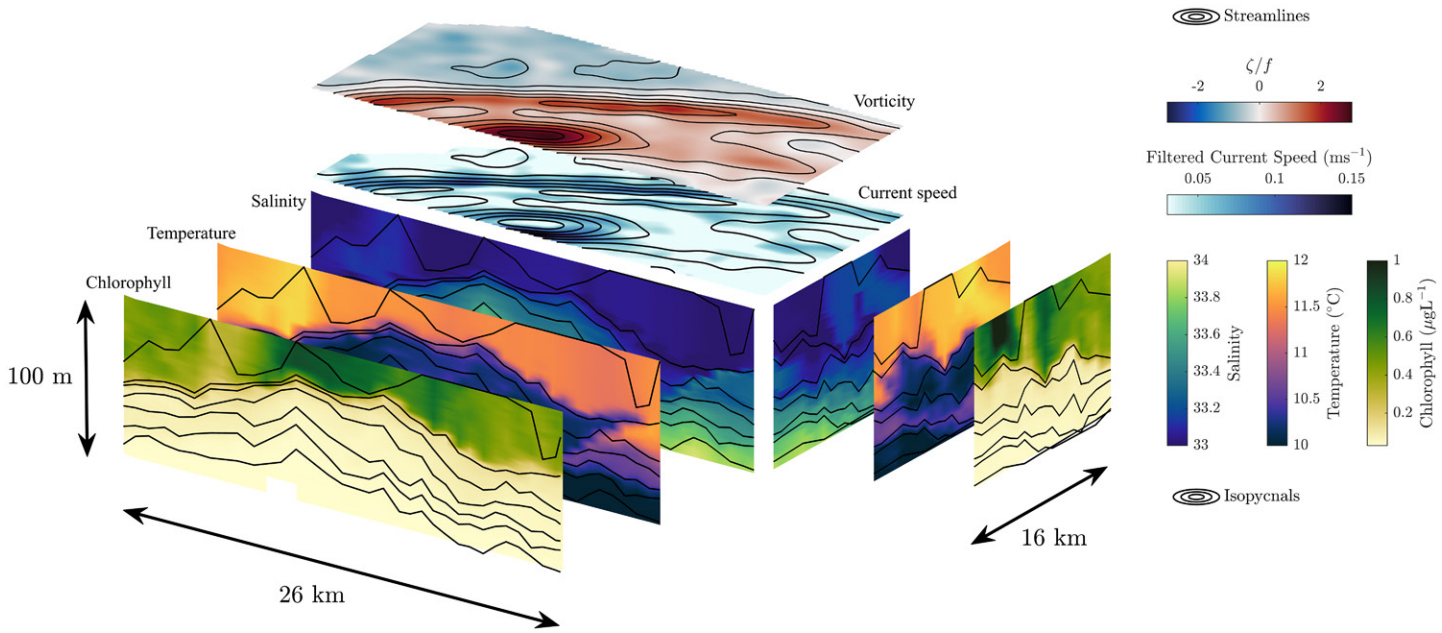

Fig. 9. Coincident hydrographic sections taken from the R/V *Sally Ride* between 0128 UTC 25 April 2023 and 0534 UTC 25 April 2023 and DopplerScatt sections taken between 2009 UTC 24 April 2023 and 2339 UTC 24 April 2023. Surface layers show vorticity ζ normalized by Coriolis frequency f and current speed for high-pass-filtered velocity fields with a filter length of 10 km, with streamlines of the high-pass-filtered velocity shown on both the vorticity and current speed. Subsurface layers show sections of salinity, temperature, and calibrated chlorophyll fluorescence. The contours in the subsurface panels indicate seawater density.

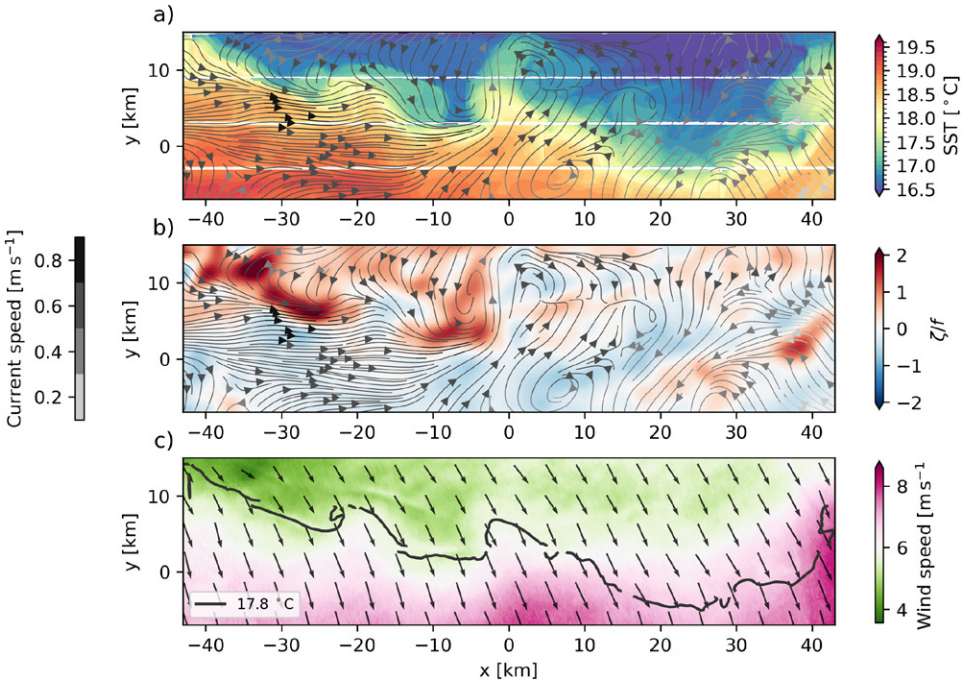

Fig. 10. (a) SST on 24 Oct 2022 from the MOSES infrared imager (colors; scene as in Fig. 6), with ocean current streamlines collected simultaneously with the DopplerScatt instrument (grayscale lines). Note the close agreement between SST and velocity structures. (b) Ocean vorticity estimated from the DopplerScatt surface currents at 2-km resolution. This is one of the first synoptic maps of ocean vorticity for testing the fidelity of model vorticity estimates like the ones shown in Fig. 2. (c) Surface wind vectors and wind speed (colors) and the 17.8°C isotherm from the MOSES infrared imager (black line). There is a close correspondence between wind speed and SST, suggesting that the submesoscale SST variations are driving wind speed variations.

these data, and we hope others will also use these datasets to extract new insights about ocean dynamics and air–sea interaction.

Acknowledgments. This work is a contribution to the S-MODE project, an EVS-3 Investigation awarded under NASA Research Announcement NNH17ZDA001N-EVS3. The success of the S-MODE field campaigns required the dedicated efforts of more than 100 people who supported the data collection at sea and in the air. We thank the captains and crews of the R/V *Oceanus*, M/V *Bold Horizon*, and R/V *Sally Ride* and the pilots and ground crew of the NASA Armstrong B200, the NASA Langley Gulfstream III, and the Twin Otter International aircraft. We thank the staff of the Earth Science Project Office at the NASA Ames Research Center for facilitating many aspects of the project, including the aircraft operations at Ames. We thank two anonymous reviewers for helpful suggestions, and we thank Professor Christine Gommenginger for an extensive and constructive review that substantially improved the manuscript.

Data availability statement. All of the S-MODE data are freely available at https://podaac.jpl.nasa.gov/S-MODE or at the DOIs listed in Table 2. The satellite sea surface temperature data shown in Figs. 5 and 7 are available at https://doi.org/10.5067/GHVRS-2PO28 and https://doi.org/10.5067/GHV20-2PO28. The computational code to reproduce Fig. 10 is available through Simoes-Sousa (2024).

References

Bruegge, C. J., G. T. Arnold, J. Czapla-Myers, R. Dominguez, M. C. Helmlinger, D. R. Thompson, J. Van den Bosch, and B. N. Wenny, 2021: Vicarious calibration of eMAS, AirMSPI, and AVIRIS sensors during FIREX-AQ. *IEEE Trans. Geosci. Remote Sens.*, **59**, 10 286–10 297, https://doi.org/10.1109/TGRS.2021.3066997.

Callies, J., and R. Ferrari, 2013: Interpreting energy and tracer spectra of upper-ocean turbulence in the submesoscale range (1–200 km). *J. Phys. Oceanogr.*, **43**, 2456–2474, https://doi.org/10.1175/JPO-D-13-063.1.

Capet, X., J. C. McWilliams, M. J. Molemaker, and A. F. Shchepetkin, 2008a: Mesoscale to submesoscale transition in the California Current system. Part I: Flow structure, eddy flux, and observational tests. *J. Phys. Oceanogr.*, **38**, 29–43, https://doi.org/10.1175/2007JPO3671.1.

——, ——, ——, and ——, 2008b: Mesoscale to submesoscale transition in the California Current System. Part II: Frontal processes. *J. Phys. Oceanogr.*, **38**, 44–64, https://doi.org/10.1175/2007JPO3672.1.

——, ——, ——, and ——, 2008c: Mesoscale to submesoscale transition in the California Current System. Part III: Energy balance and flux. *J. Phys. Oceanogr.*, **38**, 2256–2269, https://doi.org/10.1175/2008JPO3810.1.

CMEMS, 2023: Global ocean gridded L 4 sea surface heights and derived variables reprocessed 1993 ongoing. E.U. Copernicus Marine Service Information (CMEMS), Marine Data Store (MDS), accessed 15 May 2023, https://doi.org/10.48670/moi-00148.

D'Asaro, E., C. Lee, L. Rainville, R. Harcourt, and L. Thomas, 2011: Enhanced turbulence and energy dissipation at ocean fronts. *Science*, **332**, 318–322, https://doi.org/10.1126/science.1201515.

D'Asaro, E. A., 2003: Performance of autonomous Lagrangian floats. *J. Atmos. Oceanic Technol.*, **20**, 896–911, https://doi.org/10.1175/1520-0426(2003)020<0896:POALF>2.0.CO;2.

——, and Coauthors, 2018: Ocean convergence and the dispersion of flotsam. *Proc. Natl. Acad. Sci. USA*, **115**, 1162–1167, https://doi.org/10.1073/pnas.1718453115.

Dever, M., M. Freilich, J. T. Farrar, B. Hodges, T. Lanagan, A. J. Baron, and A. Mahadevan, 2020: EcoCTD for profiling oceanic physical–biological properties from an underway ship. *J. Atmos. Oceanic Technol.*, **37**, 825–840, https://doi.org/10.1175/JTECH-D-19-0145.1.

Earth Science Information Partners, 2022: Attribute Convention for Data Discovery 1-3, version 1.3. https://wiki.esipfed.org/Attribute_Convention_for_Data_Discovery_1-3#Document.

Eaton, B., and Coauthors, 2022: NetCDF Climate and Forecast (CF) metadata conventions, version 1.10. https://cfconventions.org/Data/cf-conventions/cf-conventions-1.10/cf-conventions.html.

Farrar, J., and Coauthors, 2020: S-MODE: The Sub-Mesoscale Ocean Dynamics Experiment. *IGARSS 2020—2020 IEEE Int. Geoscience and Remote Sensing Symp.*, Waikoloa, HI, Institute of Electrical and Electronics Engineers, 3533–3536, https://doi.org/10.1109/IGARSS39084.2020.9323112.

Freilich, M., L. Lenain, and S. T. Gille, 2023: Characterizing the role of non-linear interactions in the transition to submesoscale dynamics at a dense filament. *Geophys. Res. Lett.*, **50**, e2023GL103745, https://doi.org/10.1029/2023GL103745.

Fu, L.-L., and Coauthors, 2024: The Surface Water and Ocean Topography Mission: A breakthrough in radar remote sensing of the ocean and land surface water. *Geophys. Res. Lett.*, **51**, e2023GL107652, https://doi.org/10.1029/2023GL107652.

Gentemann, C., and Coauthors, 2020: Saildrone: Adaptively sampling the marine environment. *Bull. Amer. Meteor. Soc.*, **101**, E744–E762, https://doi.org/10.1175/BAMS-D-19-0015.1.

Grare, L., N. M. Statom, N. Pizzo, and L. Lenain, 2021: Instrumented wave gliders for air-sea interaction and upper ocean research. *Front. Mar. Sci.*, **8**, 664728, https://doi.org/10.3389/fmars.2021.664728.

Harlan, J., E. Terrill, L. Hazard, C. Keen, D. Barrick, C. Whelan, S. Howden, and J. Kohut, 2010: The integrated ocean observing system high-frequency radar network: Status and local, regional, and national applications. *Mar. Technol. Soc. J.*, **44**, 122–132, https://doi.org/10.4031/MTSJ.44.6.6.

Hodges, B. A., L. Grare, B. Greenwood, K. Matsuyoshi, N. Pizzo, N. M. Statom, J. Farrar, and L. Lenain, 2023: Evaluation of ocean currents observed from autonomous surface vehicles. *J. Atmos. Oceanic Technol.*, **40**, 1121–1136, https://doi.org/10.1175/JTECH-D-23-0066.1.

Jacobs, G., J. Richman, J. Doyle, P. Spence, B. Bartels, C. Barron, R. Helber, and F. Bud, 2014: Simulating conditional deterministic predictability within ocean frontogenesis. *Ocean Model.*, **78**, 1–16, https://doi.org/10.1016/j.ocemod.2014.02.004.

——, J. D'Addezio, B. Bartels, and C. DeHaan, 2023: Adapting constrained scales to observation resolution in ocean forecasts. *Ocean Modell.*, **186**, 102252, https://doi.org/10.1016/j.ocemod.2023.102252.

Johnson, L., C. M. Lee, E. A. D'Asaro, L. Thomas, and A. Shcherbina, 2020: Restratification at a California Current upwelling front. Part I: Observations. *J. Phys. Oceanogr.*, **50**, 1455–1472, https://doi.org/10.1175/JPO-D-19-0203.1.

Lenain, L., and W. K. Melville, 2017: Measurements of the directional spectrum across the equilibrium saturation ranges of wind-generated surface waves. *J. Phys. Oceanogr.*, **47**, 2123–2138, https://doi.org/10.1175/JPO-D-17-0017.1.

——, N. M. Statom, and W. K. Melville, 2019: Airborne measurements of surface wind and slope statistics over the ocean. *J. Phys. Oceanogr.*, **49**, 2799–2814, https://doi.org/10.1175/JPO-D-19-0098.1.

——, and Coauthors, 2023: Airborne remote sensing of upper-ocean and surface properties, currents and their gradients from meso to submesoscales. *Geophys. Res. Lett.*, **50**, e2022GL102468, https://doi.org/10.1029/2022GL102468.

Mahadevan, A., 2016: The impact of submesoscale physics on primary productivity of plankton. *Annu. Rev. Mar. Sci.*, **8**, 161–184, https://doi.org/10.1146/annurev-marine-010814-015912.

——, A. Pascual, D. L. Rudnick, S. Ruiz, J. Tintoré, and E. D'Asaro, 2020: Coherent pathways for vertical transport from the surface ocean to interior. *Bull. Amer. Meteor. Soc.*, **101**, E1996–E2004, https://doi.org/10.1175/BAMS-D-19-0305.1.

Marshall, J., A. Adcroft, J.-M. Campin, C. Hill, and A. White, 2004: Atmosphere–ocean modeling exploiting fluid isomorphisms. *Mon. Wea. Rev.*, **132**, 2882–2894, https://doi.org/10.1175/MWR2835.1.

McWilliams, J. C., 2016: Submesoscale currents in the ocean. *Proc. Roy. Soc.*, **472**, 20160117, https://doi.org/10.1098/rspa.2016.0117.

Melville, W. K., L. Lenain, D. R. Cayan, M. Kahru, J. P. Kleissl, P. Linden, and N. M. Statom, 2016: The Modular Aerial Sensing System. *J. Atmos. Oceanic Technol.*, **33**, 1169–1184, https://doi.org/10.1175/JTECH-D-15-0067.1.

Morrow, R., and Coauthors, 2019: Global observations of fine-scale ocean surface topography with the Surface Water and Ocean Topography (SWOT) Mission. *Front. Mar. Sci.*, **6**, 232, https://doi.org/10.3389/fmars.2019.00232.

Munk, W., L. Armi, K. Fischer, and F. Zachariasen, 2000: Spirals on the sea. *Proc. Roy. Soc. London*, **456A**, 1217–1280, https://doi.org/10.1098/rspa.2000.0560.

Novelli, G., C. M. Guigand, C. Cousin, E. H. Ryan, N. J. Laxague, H. Dai, B. K. Haus, and T. M. Özgökmen, 2017: A biodegradable surface drifter for ocean sampling on a massive scale. *J. Atmos. Oceanic Technol.*, **34**, 2509–2532, https://doi.org/10.1175/JTECH-D-17-0055.1.

O'Reilly, J. E., and P. J. Werdell, 2019: Chlorophyll algorithms for ocean color sensors-OC4, OC5 & OC6. *Remote Sens. Environ.*, **229**, 32–47, https://doi.org/10.1016/j.rse.2019.04.021.

Pujol, M.-I., Y. Faugère, G. Taburet, S. Dupuy, C. Pelloquin, M. Ablain, and N. Picot, 2016: DUACS DT2014: The new multi-mission altimeter data set reprocessed over 20 years. *Ocean Sci.*, **12**, 1067–1090, https://doi.org/10.5194/os-12-1067-2016.

Rodríguez, E., A. Wineteer, D. Perkovic-Martin, T. Gál, B. Stiles, N. Niamsuwan, and R. Monje, 2018: Estimating ocean vector winds and currents using a Ka-band pencil-beam Doppler scatterometer. *Remote Sens.*, **10**, 576, https://doi.org/10.3390/rs10040576.

——, M. Bourassa, D. Chelton, J. T. Farrar, D. Long, D. Perkovic-Martin, and R. Samelson, 2019: The winds and currents mission concept. *Front. Mar. Sci.*, **6**, 438, https://doi.org/10.3389/fmars.2019.00438.

——, A. Wineteer, D. Perkovic-Martin, T. Gál, S. Anderson, S. Zuckerman, J. Stear, and X. Yang, 2020: Ka-band Doppler scatterometry over a loop current eddy. *Remote Sens.*, **12**, 2388, https://doi.org/10.3390/rs12152388.

Rudnick, D. L., 2001: On the skewness of vorticity in the upper ocean. *Geophys. Res. Lett.*, **28**, 2045–2048, https://doi.org/10.1029/2000GL012265.

——, N. D. Zarokanellos, and J. Tintoré, 2022: A four-dimensional survey of the Almeria–Oran front by underwater gliders: Tracers and circulation. *J. Phys. Oceanogr.*, **52**, 225–242, https://doi.org/10.1175/JPO-D-21-0181.1.

Samelson, R. M., 2022: Wind drift in a homogeneous equilibrium sea. *J. Phys. Oceanogr.*, **52**, 1945–1967, https://doi.org/10.1175/JPO-D-22-0017.1.

Scully-Power, P., 1986: Navy Oceanographer Shuttle observations, STS 41-G mission report. Naval Underwater Systems Center Tech. Rep., NUSC Tech. Doc. 7611, 117 pp., https://apps.dtic.mil/sti/pdfs/ADA233578.pdf.

Shcherbina, A. Y., E. A. D'Asaro, C. M. Lee, J. M. Klymak, M. J. Molemaker, and J. C. McWilliams, 2013: Statistics of vertical vorticity, divergence, and strain in a developed submesoscale turbulence field. *Geophys. Res. Lett.*, **40**, 4706–4711, https://doi.org/10.1002/grl.50919.

——, ——, and S. Nylund, 2018: Observing finescale oceanic velocity structure with an autonomous Nortek acoustic Doppler current profiler. *J. Atmos. Oceanic Technol.*, **35**, 411–427, https://doi.org/10.1175/JTECH-D-17-0108.1.

Siegelman, L., P. Klein, P. Rivière, A. F. Thompson, H. S. Torres, M. Flexas, and D. Menemenlis, 2020: Enhanced upward heat transport at deep submesoscale ocean fronts. *Nat. Geosci.*, **13**, 50–55, https://doi.org/10.1038/s41561-019-0489-1.

Simoes-Sousa, I., 2024: NASA-SMODE/smode_bams: Initial release. Zenodo, https://doi.org/10.5281/zenodo.13942622.

Stevens, B., and Coauthors, 2021: EUREC^{4}A. *Earth Syst. Sci. Data*, **13**, 4067–4119, https://doi.org/10.5194/essd-13-4067-2021.

Stramski, D., and Coauthors, 2008: Relationships between the surface concentration of particulate organic carbon and optical properties in the eastern South Pacific and eastern Atlantic Oceans. *Biogeosciences*, **5**, 171–201, https://doi.org/10.5194/bg-5-171-2008.

Sullivan, P. P., and J. C. McWilliams, 2024: Oceanic frontal turbulence. *J. Phys. Oceanogr.*, **54**, 333–358, https://doi.org/10.1175/JPO-D-23-0033.1.

Tarry, D. R., and Coauthors, 2021: Frontal convergence and vertical velocity measured by drifters in the Alboran Sea. *J. Geophys. Res. Oceans*, **126**, e2020JC016614, https://doi.org/10.1029/2020JC016614.

——, and Coauthors, 2022: Drifter observations reveal intense vertical velocity in a surface ocean front. *Geophys. Res. Lett.*, **49**, e2022GL098969, https://doi.org/10.1029/2022GL098969.

Taylor, J. R., and A. F. Thompson, 2023: Submesoscale dynamics in the upper ocean. *Annu. Rev. Fluid Mech.*, **55**, 103–127, https://doi.org/10.1146/annurev-fluid-031422-095147.

Thomas, L. N., A. Tandon, and A. Mahadevan, 2008: Submesoscale processes and dynamics. *Ocean Modeling in an Eddying Regime*, Amer. Geophys. Union, 17–38, https://doi.org/10.1029/177GM04.

Thompson, D. R., and Coauthors, 2019: A unified approach to estimate land and water reflectances with uncertainties for coastal imaging spectroscopy. *Remote Sens. Environ.*, **231**, 111198, https://doi.org/10.1016/j.rse.2019.05.017.

——, and Coauthors, 2024: On-orbit calibration and performance of the EMIT imaging spectrometer. *Remote Sens. Environ.*, **303**, 113986, https://doi.org/10.1016/j.rse.2023.113986.

Torres, H., A. Wineteer, P. Klein, T. Lee, J. Wang, E. Rodriguez, D. Menemenlis, and H. Zhang, 2023: Anticipated capabilities of the ODYSEA wind and current mission concept to estimate wind work at the air–sea interface. *Remote Sens.*, **15**, 3337, https://doi.org/10.3390/rs15133337.

Torres, H. S., and Coauthors, 2022: Separating energetic internal gravity waves and small-scale frontal dynamics. *Geophys. Res. Lett.*, **49**, e2021GL096249, https://doi.org/10.1029/2021GL096249.

Uchida, T., and Coauthors, 2022: Cloud-based framework for inter-comparing submesoscale-permitting realistic ocean models. *Geosci. Model Dev.*, **15**, 5829–5856, https://doi.org/10.5194/gmd-15-5829-2022.

Villas Bôas, A. B., and Coauthors, 2019: Integrated observations of global surface winds, currents, and waves: Requirements and challenges for the next decade. *Front. Mar. Sci.*, **6**, 425, https://doi.org/10.3389/fmars.2019.00425.

Westbrook, E., F. M. Bingham, S. Brodnitz, J. T. Farrar, E. Rodriguez, and C. Zappa, 2024: Submesoscale Ocean Dynamics Experiment (S-MODE) data submission report. Woods Hole Oceanographic Institution Tech. Rep. WHOI-2024-03, 144 pp., https://doi.org/10.1575/1912/69362.

Wineteer, A., H. S. Torres, and E. Rodriguez, 2020a: On the surface current measurement capabilities of spaceborne Doppler scatterometry. *Geophys. Res. Lett.*, **47**, e2020GL090116, https://doi.org/10.1029/2020GL090116.

——, and Coauthors, 2020b: Measuring winds and currents with Ka-band Doppler scatterometry: An airborne implementation and progress towards a spaceborne mission. *Remote Sens.*, **12**, 1021, https://doi.org/10.3390/rs12061021.

Yu, J., C. Blain, P. Martin, and T. Campbell, 2023: Two-way nesting in a split-implicit ocean model: NCOM. *J. Atmos. Oceanic Technol.*, **40**, 865–883, https://doi.org/10.1175/JTECH-D-22-0112.1.